

Far-infrared magnetoabsorption of exciton system in silicon

Tyuzi Ohyama

Department of Physics, College of General Education, Osaka University, Toyonaka 560, Japan

(Received 5 September 1980)

In this work we report on the first observation of the far-infrared laser (84–220 μm) magneto-optical absorption by the exciton system in silicon up to the magnetic field of 50 kG and over the temperature range of 1.7–50 K. The major absorption lines observed for three geometries, $\vec{B} \parallel \langle 001 \rangle$, $\vec{B} \parallel \langle 111 \rangle$, and $\vec{B} \parallel \langle 110 \rangle$, are safely attributed to the $1s \rightarrow 2p$ -type transition of excitons. It is found that the absorption linewidth is sensitive to temperature and to impurity concentration. The magnitudes of the exciton-phonon interaction and of the exciton-impurity interaction are thereby discussed. The absorption increases markedly with temperature and increases linearly with the level of excitation, indicating the coexistence with electron-hole drops. The work function of the condensed phase is obtained through the thermodynamical method to be $\phi = 7.6$ meV. From the time-resolved experiments, the temperature dependence of the lifetime of the exciton is also obtained.

I. INTRODUCTION

While a large number of experiments¹ on the high-density exciton system in germanium have been performed through microwave measurements, recombination spectra, light scattering, ultrasonic attenuation, far-infrared magneto absorption, etc., the main probe for investigating the excitonic system in silicon has so far been restricted only to recombination spectra.^{1,2} Application of an external magnetic field for observing the induced changes of the electronic energy levels has been one of the basic approaches in solid-state spectroscopy, and information about the exciton system in silicon should be greatly enhanced through the use of magneto optics. The far-infrared laser magneto absorption,^{3–5} which is a powerful tool for studying the internal structure of the exciton, has indeed been used to make a direct observation of the dynamical properties of excitons in germanium. Though no comparable experiment exists for silicon, some practical information is the band-edge absorption provided by Shaklee and Nahory,⁶ who gave the $1s$ to $2p$ separation to be 10.7 and 11.0 meV for TA- and LA-phonon-assisted transitions, respectively. These energies correspond to the far-infrared region around the wavelength of 100 μm . In the absence of a magnetic field, moreover, Timusk *et al.*⁷ have recently furnished new experimental information of the $1s - 2p$ -type transitions of excitons in silicon. In this work we report on the first observation of the far-infrared laser magneto absorption of excitons in silicon, which leads to some important conclusions about their dynamical properties.

II. EXPERIMENTAL PROCEDURES

Experiments are performed on one undoped ($N_A - N_D \approx 10^{12} \text{ cm}^{-3}$), three boron-doped ($N_B = 8.0 \times 10^{13} \text{ cm}^{-3}$, $N_B = 4.3 \times 10^{14} \text{ cm}^{-3}$, $N_B = 2.0 \times 10^{15} \text{ cm}^{-3}$), and two phosphorus-doped ($N_P = 8.8 \times 10^{13} \text{ cm}^{-3}$, $N_P = 8.0 \times 10^{14} \text{ cm}^{-3}$) silicon crystals. All the samples are rectangular shaped, having typical dimensions of $4 \times 4 \times 3 \text{ mm}^3$. For the far-infrared source, the wavelengths of 119 and 220 μm are obtained from a discharge-type H_2O laser, 84 μm from a discharge-type D_2O laser, and 96.5 μm (CH_3OH) and 103 μm (CH_3OD) are obtained from a CO_2 laser-pumped laser, all of which are operated in pulses at the repetition of 30 Hz in synchronized combination with the photoexcitation light pulses at 15 Hz. The excitation light is provided by a xenon flash lamp having the pulse width of $\sim 1 \mu\text{s}$. The lamp yields the maximum total discharge energy of 0.24 J per pulse, but the low duty ratio prevents temperature rise by the excitation light. The excitation light is guided through a self-focused light guide (SELFOC) provided by the Nippon Sheet Glass Co., Ltd. The signal is detected by an n -type InSb Putley detector that uses a persistent current solenoid and a wide-band amplifier with a response time shorter than 1 μs .

Experiments are carried out in the Faraday configuration, and a magnetic field up to 50 kG is applied along the $\langle 001 \rangle$, $\langle 111 \rangle$, and $\langle 110 \rangle$ crystallographic axes for the undoped silicon and along a $\langle 111 \rangle$ axis for doped samples. Temperature is varied between 1.7 and 50 K. A heater wound outside the brass tube transmitting the far-infrared beam is used to raise the temperature of the sample to a desired temperature above 4.2 K. Temperature is measured by a Au-Fe versus Chromel

thermocouple pressed onto the sample holder and can be controlled with a feedback system to an accuracy of the order of 0.1 K.

The absorption spectra are obtained as $\ln(I_0/I_L)$, employing two boxcars with the common aperture of $0.5 \mu\text{s}$. Here I_L and I_0 are the intensities of the transmitted far-infrared laser beams at the same delay time, with and without optical excitation. The observed signal is then proportional to the absorption coefficient by the optically induced system. As the apertures of the boxcars are narrower than the pulse width of the excitation light and shorter than the apparent lifetime of excitons, we proceed by assuming a steady state at the time under illumination of the excitation light. The other details are the same as described elsewhere.⁴

III. ZEEMAN EFFECT OF EXCITONS

In order to get the information about the excitonic states in the presence of an external magnetic field, realistic exciton models and their accurate description are necessary. Some simple calculations of the magnetic field dependence of the excitonic energy levels have been available for many years.⁸⁻¹⁰ The simplest description is based on the nondegenerate, parabolic, and isotropic two-band model. Recently, considerable progress has been made in the calculation of the effects of an

external field on the lower excitonic states for degenerate bands.¹¹

In the effective-mass approximation and in the isotropic two-band model, we obtain the simple Schrödinger equation in which three magnetic terms appear. When the magnetic energy $\hbar\omega_c$ is much smaller than the Coulomb binding energy E_{ex} (this condition is satisfied for the excitonic state in silicon, rigorously speaking, at the magnetic field lower than 400 kG), they are the linear Zeeman term, the diamagnetic term, and the magneto-Stark term introduced by Hopfield and Thomas.⁹

Figure 1 shows the typical spectra from the undoped sample observed at 4.2 K for several wavelengths and at the geometry of $\vec{B} \parallel \langle 111 \rangle$. The spectra observed at 1.7 K for three different geometries, $\vec{B} \parallel \langle 001 \rangle$, $\vec{B} \parallel \langle 111 \rangle$, and $\vec{B} \parallel \langle 110 \rangle$, but for the fixed wavelength of $119 \mu\text{m}$, are shown in Fig. 2. The major absorption lines show a little anisotropy, and the positions strongly depend on the wavelength of the laser. Moreover, the Zeeman absorption lines can be observed only in the limited region of the wavelength. For example, we have no absorption signal for $146 \mu\text{m}$ (8.5 meV), which shows that the first excited state exists at an energy higher than 8.5 meV. For $84 \mu\text{m}$ (14.8 meV), a nonresonant absorption is observed which originates in the photoionization of excitons into

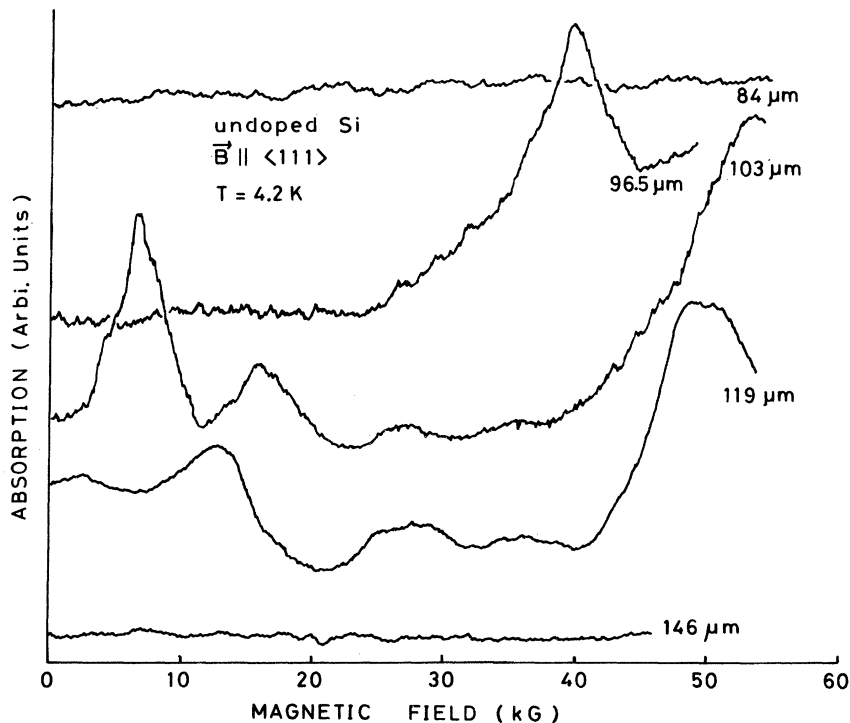


FIG. 1. Magnetoabsorption traces at 4.2 K for the wavelength of 84, 96.5, 103, and $146 \mu\text{m}$ and for $\vec{B} \parallel \langle 111 \rangle$.

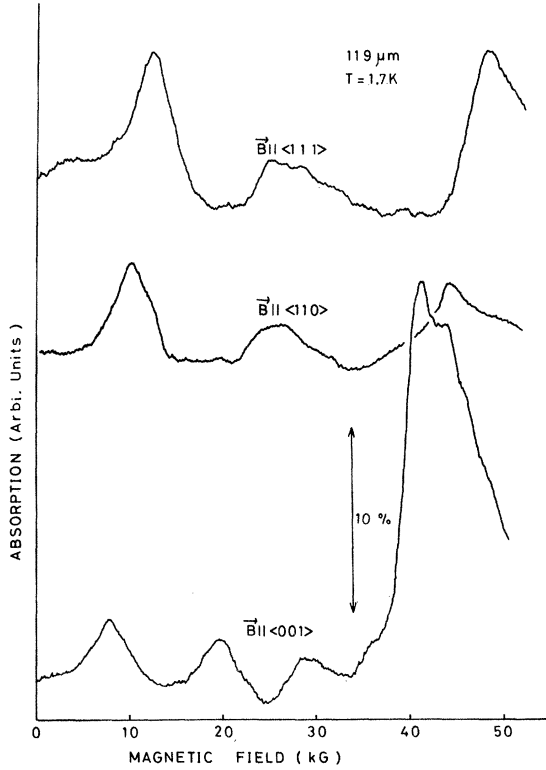


FIG. 2. Typical magnetoabsorption spectra at 1.7 K observed for the wavelength of $119 \mu\text{m}$ and for $\vec{B} \parallel \langle 110 \rangle$, $\vec{B} \parallel \langle 111 \rangle$, and $\vec{B} \parallel \langle 001 \rangle$.

free pairs. In Fig. 3 we locate a limited number of points which correspond to the peaks of the excitonic Zeeman absorption and give the corresponding energy curves against the magnetic field for the geometry of $\vec{B} \parallel \langle 111 \rangle$. A global feature of the

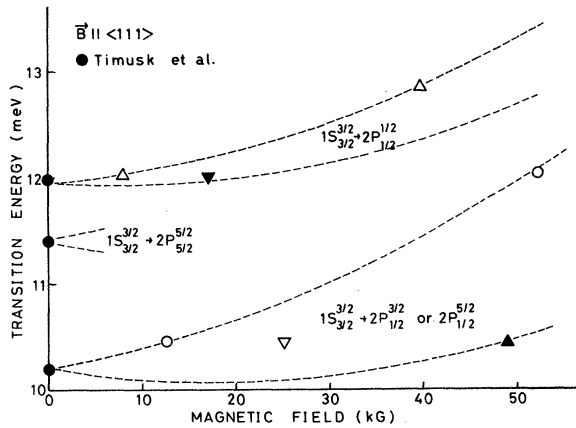


FIG. 3. Transition energies of the excitonic Zeeman absorption lines against magnetic field in $\vec{B} \parallel \langle 111 \rangle$. Solid circles at zero magnetic field denote the data by Timusk *et al.* (Ref. 7). The broken lines represent the calculation with our proper parameters according to Eq. (4) (see text).

excitonic energy-level variation with magnetic field is obvious here, suggesting that the excitonic energy levels in silicon change gradually over the magnetic field (the changes are also shown in the figure). In silicon the binding energy of the exciton is about 15 meV, which is about one-third of the estimated spin-orbit splitting of the valence band. All valence bands may therefore make a significant contribution to the excitonic state. On account of this, Lipari and Altarelli¹² show that one will have two 1s-like ground states and at least six possible series states for the 2p state at zero magnetic field. In the presence of a magnetic field, accordingly, it becomes too complicated to calculate the energy for real excitonic states.

In order to explain the observed spectra for germanium, Button *et al.*¹³ introduce a phenomenological Zeeman energy of the form

$$E = D(J_z^2 - J^2/3) + \beta(g_e S - g_h J_z)B + cB^2, \quad (1)$$

where J is the total angular momentum of the hole, S is the spin of the electron, and β is the Bohr magneton.

The effective g value for any given exciton state will then be of the form¹⁴

$$g_{\text{eff}} = a_\mu g_\mu + a_e g_e + a_h g_h, \quad (2)$$

where a_i 's ($i = \mu, e, h$) are numerical coefficients which depend on the symmetries of the electron, hole, and envelope functions. In the presence of appreciable spin-orbit coupling, Lipari and Altarelli¹² express the wave function in the F, F_z representation, where $F (= L + J)$ is the composition of the orbital angular momentum of the envelope function and the spin $\frac{3}{2}$ corresponding to the valence-band degeneracy, while F_z is its projection on the magnetic field direction. Accordingly, the effective g value will be of the form

$$g_{\text{eff}}^F = a_e g_e + a_F g_F. \quad (3)$$

Hereafter we will adopt the F, F_z representation in the excitonic states.

If we write ΔE for the transition energy from 1s to 2p, its form must bear some analogy with Eq. (1), namely,

$$\Delta E = a^F \pm b^F F_z B + c^F F_z^2 B^2. \quad (4)$$

As the selection rules for the electric-dipole transitions in the Faraday configuration must be $\Delta S = 0$ and $\Delta F_z = \pm 1$, the explicit form for the transition energy is expressed only in terms of F and F_z , and the (\pm) signs in Eq. (4) refer to the transition for $\Delta F_z = \pm 1$, respectively. The first term in Eq. (4) represents the zero-field splitting, the second represents the difference in Zeeman energy of the hole for 1s and 2p excitonic states, respec-

tively, and the third represents a diamagnetic contribution which becomes dominant above 20 kG. Out of many possible excitonic transitions, we have tried to obtain values of the coefficients for the transition from the lowest excitonic state $1S_{\pm 3/2}^{3/2}$ (Ref. 7) by fitting our experimental data for $\vec{B} \parallel \langle 111 \rangle$ with the above formula. They are $b_{F_z}^F = (0.62 \times 10^{-2})$ meV/kG for $1S_{\pm 3/2}^{3/2} \rightarrow 2P_{\pm 1/2}^{1/2}$, (1.5×10^{-2}) meV/kG for $1S_{\pm 3/2}^{3/2} \rightarrow 2P_{\pm 1/2}^{3/2}$ or $1S_{\pm 3/2}^{3/2} \rightarrow 2P_{\pm 1/2}^{5/2}$, and $c_{F_z}^F = (4.1 \times 10^{-4})$ meV/kG². For other transitions, we have been unable to give the corresponding coefficients. As for the diamagnetic coefficient $c_{F_z}^F$, we find the same value for each transition. It is true that a detailed interpretation of the coefficients of the phenomenological Zeeman energy would also be possible in terms of the effective-mass approximation. However, in that case it may also be necessary to include other anisotropic terms in the Zeeman Hamiltonian. Qualitatively, our experimental results for anisotropy can be explained by inclusion of the type such as the second and third terms of Eq. (1).

IV. LINEWIDTH OF EXCITON ZEEMAN ABSORPTION

The exciton will have a fairly short lifetime against scatterings which drive the exciton into other excitonic states. Such scatterings will affect

the linewidth of the far-infrared Zeeman absorption for excitons. It should be noted that the scattering may occur both by phonons and by impurities. The linewidths ΔB of the absorption have been studied as a function of temperature and concentration of impurities.

A. Phonon scattering

Typical traces of the far-infrared magnetoabsorption by an undoped sample are shown in Fig. 4 for the wavelength of 119 μm and $\vec{B} \parallel \langle 001 \rangle$ at various temperatures. Out of many excitonic Zeeman transitions arising from the $1s \rightarrow 2p$ -type transition we take the line showing up at 45 kG as the monitoring signal for the temperature dependence of the linewidth, since the line is clearly observed even at relatively high temperatures. The linewidth broadens rapidly as the temperature is raised and the absorption intensity markedly increases. The linewidth, however, depends neither on the excitation levels nor on the delay time after the excitation. In other words, the width is not dominated by exciton-exciton scatterings but by exciton-phonon scatterings for the undoped sample. In carrying out the linewidth measurements, we make two different assumptions. First, the absorption lineshape is Lorentzian, and second, the energy shift of the excitonic level has a linear

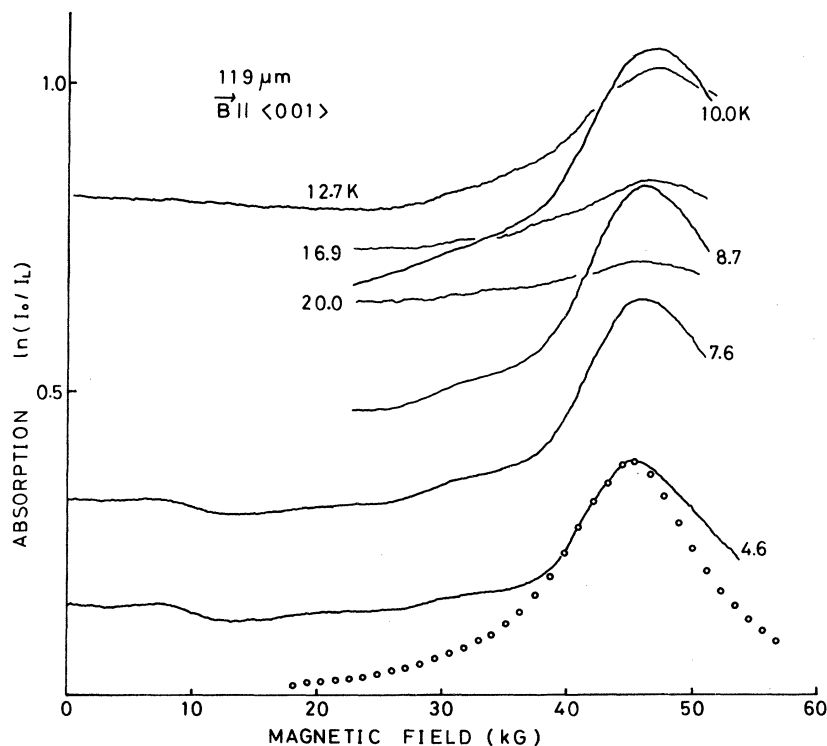


FIG. 4. Temperature dependence of magnetoabsorption spectra measured at 119 μm for $\vec{B} \parallel \langle 001 \rangle$. The absorption signal at low magnetic fields looks like a plateau. It consists of more than one broad exciton absorption. The curve shown by the open circles is the absorption calculated according to the Lorentzian shape with $\Delta B = 14$ kG.

dependence on magnetic field for the resonance interval.

The temperature dependence of the half-width ΔB is shown in Fig. 5 in logarithmic scales. It should be noted that the half-width ΔB increases roughly linearly with the temperature above 5 K. Below 5 K, it tends to be independent of temperature. The linear dependence of the half-width on the temperature agrees with Toyozawa's theory¹⁵ and indicates that the broadening of the excitonic absorption line for the undoped silicon may be due mainly to exciton-phonon interaction. Most noticeable is the decrease of temperature dependence of the half-width below 5 K. This phenomenon, which also follows from the theory, indicates that at low temperatures the scattering lifetime of excitons is mainly determined by their spontaneous emission of phonons.

Toyozawa¹⁵ gives an expression of the intraband scattering rate for 1s excitons by acoustical phonons, at temperatures higher than the characteristic temperature Θ_0 , as follows:

$$1/\tau_{\text{ex-ph}} = 8m_{\text{ex}}^{*2}kT(C_v - C_c)^2/9\pi\hbar^4\rho u, \quad (5)$$

where $m_{\text{ex}}^* = m_e^* + m_h^*$, ρ is the density of the crystal, u is the sound velocity, and C_v and C_c are the deformation potentials of the valence and the conduction bands, respectively. Equation (5) predicts that the scattering rate $1/\tau_{\text{ex-ph}}$ is proportional to temperature. This relation fails at very low temperatures where $T < \Theta_0$. In the same expression one should then replace T with Θ_0 . The characteristic temperature Θ_0 is given by

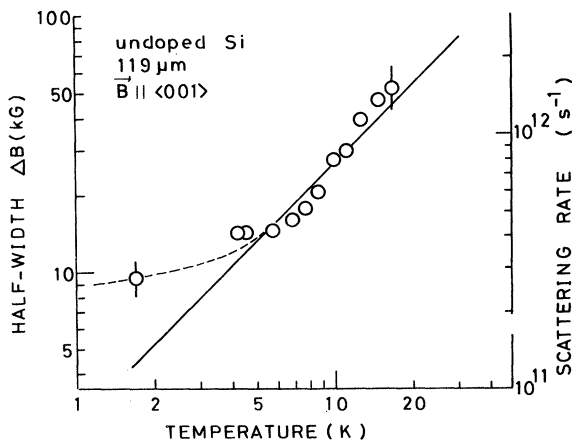


FIG. 5. Experimental results for the temperature dependence of the half-width of the excitonic Zeeman absorption line in the undoped silicon. The scattering rates derived from the line-shape analysis are also shown (see the scale on the right). The solid straight line having the slope of 45° indicates the linear dependence of the scattering rate on temperature.

$$\Theta_0 \approx 2m_{\text{ex}}^*u^2/k. \quad (6)$$

Inserting $m_{\text{ex}}^* \approx 0.6m_0$ and $u \approx 5 \times 10^5$ cm/s for silicon, we get $\Theta_0 \approx 2$ K.

From an above-mentioned knowledge of the slope of the line in meV/kG, the energy width of the line can be deduced from the experimentally determined magnetic field width. Typically, the value $\Delta B = 39$ kG obtained from our experiment at 13 K corresponds to $\Delta E \approx 0.98$ meV. Expressed in terms of collision frequency through the relation $\Delta E = \hbar/\tau$, it becomes 1.5×10^{12} s⁻¹. This result should be compared with $\Delta E = 0.5$ meV obtained by Timusk *et al.*⁷ at 13 K from the far-infrared exciton absorption at zero magnetic field. According to Toyozawa's calculation,¹⁵ the scattering rate $1/\tau_{\text{ex-ph}}$ in Eq. (5) gives 7×10^9 s⁻¹ at 13 K, if one takes $m_{\text{ex}}^* = 0.6m_0$, $\rho = 2.3$ g/cm³, $u = 5 \times 10^5$ cm/s, and $C_v - C_c = 5$ eV. This value is too small to explain the experimental result. One probable reason for the discrepancy would be that Eq. (5) is concerned only with the intraband scattering of 1s excitons, whereas the experimentally

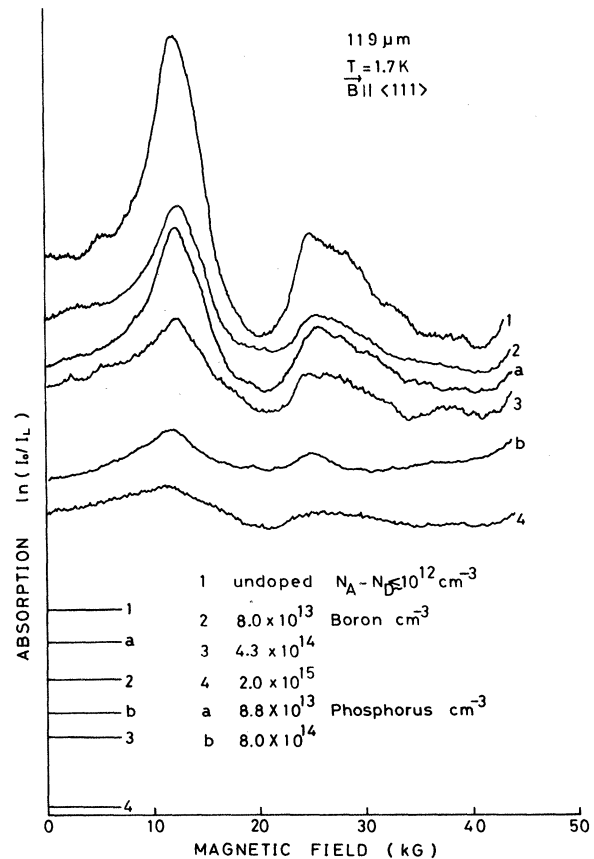


FIG. 6. Absorption lines for various impurity concentrations at 1.7 K and for the wavelength of 119 μm . The base line for each trace is also shown.

observed linewidth may be due to both intra- and interband scatterings. If this reasoning is correct, the observed line broadening of the exciton absorption should be due to the sum of two bandwidths, i.e., those of $1s$ and $2p$. Especially for $2p$ states, the interband scattering of the $2p$ exciton to $1s$ states will make a predominant contribution to the linewidth because, in addition to acoustic phonons, all other modes of lattice vibration could contribute to this scattering. Another possible origin of the line broadening may be the magneto-Stark effect due to the thermal motion of excitons in the presence of a magnetic field. But this is far from accounting for the entire broadening.

B. Impurity scattering

Typical traces of the far-infrared magneto absorption from boron-doped as well as phosphorus-doped samples at 1.7 K are shown in Fig. 6 for the wavelength of $119 \mu\text{m}$ and for $\vec{B} \parallel \langle 111 \rangle$. We take the line showing up at 12.3 kG as the monitoring signal for the linewidth measurement. We have looked for a correlation between the half-width ΔB and the impurity concentration. The results are exhibited in Fig. 7 against boron and phosphorous concentration, simultaneously. The genuine contribution of impurities to the linewidth, which we shall denote with ΔB_I , should be sought after subtracting the effect of phonon scatterings obtained from the data of undoped sample, and is given by triangles. The proportionality of

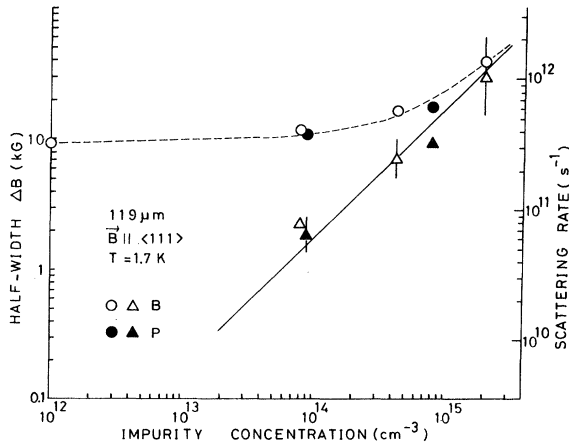


FIG. 7. Concentration dependence of the half-width for boron and phosphorus impurities. The scattering rates derived from the line-shape analysis are also shown (see the scale on the right). Triangles represent the results after subtraction of the contribution from the phonon scattering. The solid straight line having the slope of 45° shows the linear dependence of the scattering rate on the impurity concentration.

ΔB_I to N_B and N_P shows that the observed effect really reflects the scattering by doped impurities within the limits of errors involved. It should be noted that the cross section of the exciton-impurity scattering does not depend on the type of dopant, i.e., neither donor nor acceptor.

Recently, Elkomoss and Nikitine¹⁶ have calculated the exciton-neutral impurity elastic-collision cross section. The interaction potential U between the exciton in the $1s$ state and a neutral impurity can be considered to be of the van der Waals type,

$$U = -C/R^6, \quad (7)$$

where C is the van der Waals constant and R is the distance between the centers of the two neutral particles. With the collision damping theory by Weisskopf,¹⁷ the cross section is given by

$$\sigma_I = \pi(3\pi C/8v_{\text{ex}})^{2/5}, \quad (8)$$

where v_{ex} is the average velocity of excitons. Treating the van der Waals interaction as a perturbation, it can be shown that

$$C = 24E_{\text{ex}}\alpha_{\text{ex}}^3\alpha_I^3/[\hbar(1 + \alpha_I/\alpha_{\text{ex}})], \quad (9)$$

where E_{ex} is the binding energy of the exciton, and α_{ex} and α_I are Bohr radii of the exciton and the impurity, respectively. Since the Bohr radius is nearly the same for donor and acceptor, it is not too surprising that the scattering cross section apparently does not depend on the type of impurity. The experimental data can be approximated by the simple relation

$$\Delta B = \Delta B_{\text{ex-ph}} + \Delta B_I. \quad (10)$$

Here ΔB is the total observed linewidth and ΔB_I is expressed in terms of the impurity concentration N ,

$$\Delta B_I = \alpha N, \quad (11)$$

where α is a constant. $\Delta B_{\text{ex-ph}}$ is then the residual width as $N \rightarrow 0$. Thus the scattering coefficient $\alpha = \langle v_{\text{ex}} \sigma_I \rangle$, obtained from the experimental results, is $6.1 \times 10^{-4} \text{ cm}^3/\text{s}$. Taking $v_{\text{ex}} = (3kT/m_{\text{ex}}^*)^{1/2} \approx 10^6 \text{ cm/s}$ at 1.7 K, we get $\sigma_I = 5.6 \times 10^{-10} \text{ cm}^2$ as the exciton-impurity scattering cross section at this temperature. Equation (8) gives the exciton-impurity scattering cross section

$$\sigma_I = 1.1 \times 10^{-12} \text{ cm}^2. \quad (12)$$

Here we take $E_{\text{ex}} = 14.7 \text{ meV}$, $\alpha_{\text{ex}} = 41 \text{ \AA}$, $\alpha_I = 13 \text{ \AA}$, and $v_{\text{ex}} = 10^6 \text{ cm/s}$ at 1.7 K. This value is again too small to explain the experimental result. The situation, however, will be the same as the case for the exciton-phonon interaction. In fact, we need the scattering cross section for the $2p$ exciton.

V. THERMODYNAMICAL DETERMINATION OF WORK FUNCTION FOR ELECTRON-HOLE DROP

As already shown in Fig. 4, the excitonic absorption behavior strongly depends on temperature at relatively high excitation levels. That is a characteristic feature of excitons coexisting with electron-hole drops. Figure 8 shows the dependence of the absorption coefficient, obtained at the wavelength of $119 \mu\text{m}$ and at $B=0$, on the reciprocal temperature at different excitation levels. For the wavelength of $119 \mu\text{m}$ (10.4 meV), there is a resonant absorption by excitons which corresponds to $1s \rightarrow 2p$ -type transitions even at $B=0$. It is seen in Fig. 8 that, starting with a certain threshold temperature T_{th} , the absorption decreases sharply. This behavior of the absorption at $B \neq 0$ is in analogous fashion. It should be noted that the vertical axis $\ln(I_0/I_L)$ is proportional to the total exciton concentration. The straight line drawn through the threshold points, indicated with cross marks, separates the diagram into two

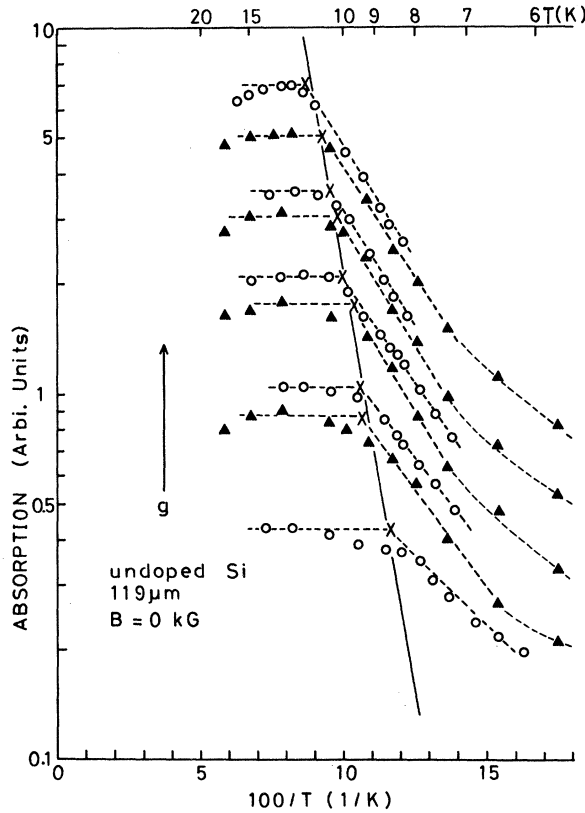


FIG. 8. Temperature dependence of the excitonic absorption intensity at different excitation levels g . Crosses represent the threshold points derived from our measurements. The solid straight line drawn through the crosses yields the value of the work function $\phi = 7.6 \text{ meV}$ according to Eq. (17) (see text).

parts: one corresponding to the region in which the exciton system is in the gas phase and the other to the liquid and gas coexisting phase. The slope of the boundary line yields the value of the work function for the electron-hole drop. In order to get a more analytical expression for the phase boundary, we will use the following simple model. The exciton flow entering the surface of the drop is given by $\pi R^2 v_{\text{ex}} n_{\text{ex}}$, where R is the radius of the drop. In steady state, this quantity must be equal to the sum of the recombination rate inside the drop and the time rate of excitons evaporating from the surface of the drop. One can write

$$\pi R^2 v_{\text{ex}} n_{\text{ex}} = 4\pi R^3 n_0 / 3\tau_0 + 4\pi R^2 A \exp(-\phi/kT). \quad (13)$$

Here τ_0 is the total recombination time, n_0 is the concentration of carrier pairs in the electron-hole drop, ϕ is the work function, and A is the coefficient inherent to the thermoionic emission which is proportional to T^2 . On the other hand, under steady-state conditions we have

$$g = n_{\text{ex}} / \tau_{\text{ex}} + 4\pi R^3 n_0 N_d / 3\tau_0, \quad (14)$$

where g is the excitation level, τ_{ex} is the lifetime of excitons, and N_d is the concentration of drops. From Eqs. (13) and (14) we obtain

$$g - (4A/v_{\text{ex}}\tau_{\text{ex}}) \exp(-\phi/kT) = (4n_0/3v_{\text{ex}}\tau_0)(1/\tau_{\text{ex}} + N_d v_{\text{ex}} \pi R^2)R. \quad (15)$$

Equation (15) tells us that $R \geq 0$ if

$$g - (4A/v_{\text{ex}}\tau_{\text{ex}}) \exp(-\phi/kT) \geq 0. \quad (16)$$

It follows that the condensed phase can appear only if the threshold value of the excitation level is reached, viz.,

$$g_{\text{th}} = (4A/v_{\text{ex}}\tau_{\text{ex}}) \exp(-\phi/kT_{\text{th}}). \quad (17)$$

The solid line in Fig. 8 corresponds to Eq. (17) with $\phi = 7.6 \text{ meV}$. Strictly speaking, the thermodynamical measurement of the work function ϕ must take into account the temperature dependence of ϕ and the effect due to the surface tension. The magnitude of the correction $2\sigma/n_0R$ to the work function is about 0.15 meV for the small drop of the radius $R = 1000 \text{ \AA}$, where σ is the surface tension. This value is smaller than the experimental error. It should be mentioned here that Dite *et al.*¹⁸ have also determined the work function through the thermodynamical method and found $\phi = 7.9 \text{ meV}$. Our result $\phi = (7.6 \pm 0.5) \text{ meV}$ will have to be compared with the spectroscopic value of 8.2 meV .¹⁹ As in the case of germanium, it cannot be avoided that a small discrepancy exists between spectroscopic and thermodynamical values of ϕ .

VI. EXCITONS COEXISTING WITH FREE CARRIERS

Figure 9 shows the absorption coefficient by excitons for $119 \mu\text{m}$ as a function of the reciprocal temperature at high excitation levels and in the midst of the excitation. In the same figure, the free-carrier absorption obtained at $220 \mu\text{m}$ is also shown under the same excitation conditions. It should be noted that the exciton absorption gradually increases as the temperature is raised, reaches the maximum at 15 K, and then decreases. The free-carrier absorption, on the other hand, drastically increases above 15 K. These phenomena suggest that a plasma composed of free electrons and holes in thermal equilibrium with excitons exists above 15 K. An essential requirement for the existence of a kind of chemical equilibrium between excitons and free carriers is that the common thermalization time is short com-

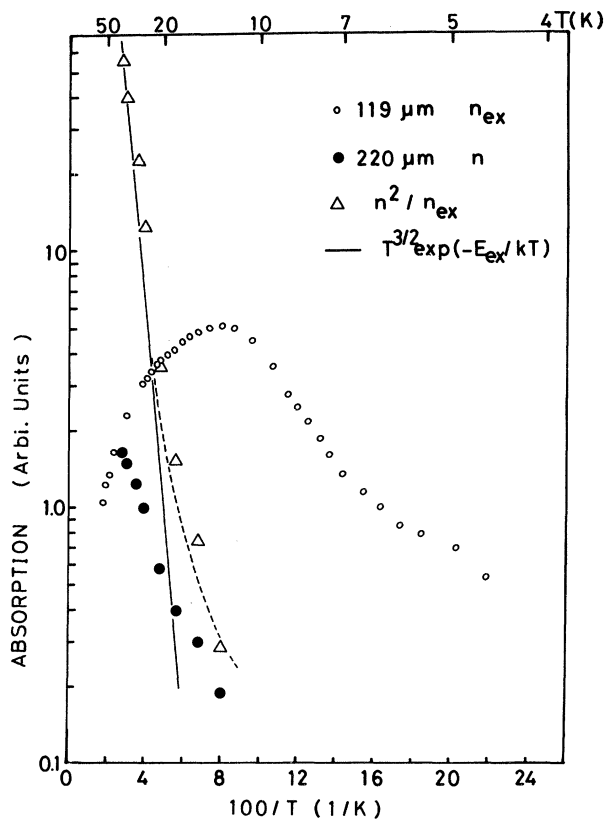


FIG. 9. Temperature dependence of the excitonic ($119 \mu\text{m}$) as well as the free-carrier ($220 \mu\text{m}$) absorption showing the dissociation of excitons to free carriers at higher temperatures. Triangles show the value $K = n^2/n_{\text{ex}}$ derived from the absorption intensity at each temperature. The solid straight line drawn through triangles at the higher-temperature region yields $E_{\text{ex}} = 14.7 \text{ meV}$ and predicts a quasiequilibrium between the exciton and the free-carrier system.

pared to the particle lifetimes. The condition is

$$Z_e Z_h / Z_{\text{ex}} = n_e n_h / n_{\text{ex}} = K(T), \quad (18)$$

where Z_e , Z_h , and Z_{ex} are the partition functions, while n_e , n_h , and n_{ex} are the total numbers of electrons, holes, and excitons, respectively, and $K(T)$ is the equilibrium constant. $K(T)$ is given by

$$K(T) = (g_e g_h / g_{\text{ex}}) (m_e^* m_h^* / 2 \hbar^2 m_{\text{ex}}^*)^{3/2} (kT)^{3/2} \times \exp(-E_{\text{ex}}/kT), \quad (19)$$

where g_e , g_h , and g_{ex} are degeneracy factors of electrons, holes, and excitons, respectively. The hole concentration in our pure sample will be equal to the electron concentration, i.e., $n_e = n_h = n$. The steep solid line in Fig. 9 gives $K(T) = n^2(T)/n_{\text{ex}}(T)$ with the exciton binding energy of 14.7 meV, which is in agreement with optical measurements. We can conclude from the experiments described above that intersystem thermalization occurs quite rapidly in comparison with the recombination times, and even at the highest exciton density reached in our experiment there is no evidence of an insulator-metal transition.²⁰

From the time-resolved experiments we have obtained the temperature dependence of the lifetime of excitons. Figure 10 shows the decay curves of excitons, obtained from the absorption at $119 \mu\text{m}$ with temperature as parameter. At higher temperatures it seems that we have two time

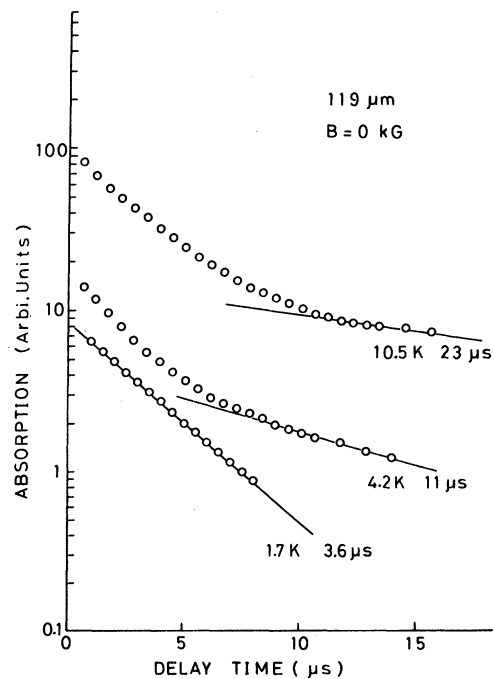


FIG. 10. Time variation of the zero-field excitonic absorption at the wavelength of $119 \mu\text{m}$ is shown for three temperatures.

constants. The initial fast decay may be due to the Auger recombination among excitons, and the subsequent slower decay, which depends on temperature, is considered to originate in the recombination via impurities. It is found that this slow decay constant reaches 30 μ s above 20 K.

VII. CONCLUSIONS

The excitonic energies of silicon in the magnetic field are obtained from the magneto absorption of several far-infrared laser wavelengths. It is found that the diamagnetic term gives a dominant contribution to the energy shift above 20 kG.

We have measured the temperature dependence of the exciton scattering rate through the linewidth measurement of the Zeeman line for various samples. Temperature dependence of the linewidth for the undoped sample and comparison of the results between the doped and undoped samples strongly indicate that the exciton-phonon scattering mainly contributes to the linewidth of the excitonic Zeeman line of the undoped sample. The existing theory by Toyozawa for the 1s exciton, however, is not quantitatively to account for the observed linewidth. A better agreement is expected if one includes the effect of the interband scattering for

the 2p exciton in the theory. For doped samples, on the other hand, the linewidth seems to consist of two effects, i.e., exciton-phonon and exciton-impurity interactions. The exciton-impurity scattering can be treated theoretically as one type of the van der Waals interaction, and it is experimentally confirmed that the scattering cross section is common for both donor and acceptor.

We obtain the work function for the electron-hole drop in silicon through the saturation effects of the exciton absorption. This is a new determination of the work function for the electron-hole drop in silicon by the thermodynamical method. We further interpreted the coexistent system composed of excitons and free electron-hole plasma in terms of the chemical-equilibrium concept.

ACKNOWLEDGMENTS

The author deeply appreciates the useful discussions with Professor E. Otsuka and Dr. H. Nakata. Dr. Nakata's kind operation of the optically pumped far-infrared laser is particularly acknowledged. The author further expresses sincere thanks to Mr. K. Enjouji of Nippon Sheet Glass Co., Ltd., for his offering of the SELFOC.

- ¹For a recent extensive review, see J. C. Hensel, T. G. Phillips, and G. A. Thomas, *Solid State Physics*, edited by H. Ehrenreich, D. Turnbull, and F. Seitz (Academic, New York, 1978), Vol. 32.
- ²Ya. Pokrovskii, *Phys. Status Solidi A* **11**, 385 (1972).
- ³K. Fujii and E. Otsuka, *J. Phys. Soc. Jpn.* **38**, 742 (1975).
- ⁴E. Otsuka, T. Ohyama, H. Nakata, and Y. Okada, *J. Opt. Soc. Am.* **67**, 931 (1977).
- ⁵K. Muro and Y. Nisida, *J. Phys. Soc. Jpn.* **40**, 1069 (1976).
- ⁶K. L. Shaklee and R. E. Nahory, *Phys. Rev. Lett.* **24**, 942 (1970).
- ⁷T. Timusk, H. Navarro, N. O. Lipari, and M. Altarelli, *Solid State Commun.* **25**, 217 (1978).
- ⁸R. J. Elliot and R. Loudon, *J. Phys. Chem. Solids* **25**, 59 (1964).
- ⁹J. J. Hopfield and D. G. Thomas, *Phys. Rev.* **122**, 35 (1961).
- ¹⁰D. Bimberg, *Advances in Solid State Physics* (Perga-

- mon, New York, 1977), Vol. XVII, p. 195.
- ¹¹N. O. Lipari and A. Baldereschi, *Phys. Rev. B* **3**, 2497 (1971); **6**, 3764 (1972).
- ¹²N. O. Lipari and M. Altarelli, *Solid State Commun.* **18**, 951 (1976).
- ¹³K. J. Button, L. M. Roth, W. H. Kleiner, S. Zwerdling, and B. Lax, *Phys. Rev. Lett.* **2**, 161 (1969).
- ¹⁴R. S. Knox, *Theory of Excitons*, Suppl. 5 of *Solid State Physics* (Academic, New York, 1963), p. 83.
- ¹⁵Y. Toyozawa, *Prog. Theor. Phys.* **20**, 53 (1958).
- ¹⁶S. G. Elkomoss and S. Nikitine, *J. Phys. Chem. Solids* **41**, 413 (1980).
- ¹⁷V. F. Weisskopf, *Z. Phys.* **75**, 287 (1932).
- ¹⁸A. F. Dite, V. D. Kulakovskii, and V. B. Timofeev, *Zh. Eksp. Teor. Fiz.* **72**, 1156 (1977) [*Sov. Phys.—JETP* **45**, 604 (1977)].
- ¹⁹R. B. Hammond, T. C. McGill, and J. W. Mayer, *Phys. Rev. B* **13**, 3566 (1976).
- ²⁰N. F. Mott, *Metal-Insulator Transitions* (Taylor and Francis, London, 1974).